

Contribution from Rockwell International,
Rocky Flats Plant, Golden, Colorado 80401

XPS–AES Characterization of Plutonium Oxides and Oxide Carbide. The Existence of Plutonium Monoxide

D. T. LARSON and JOHN M. HASCHKE*

Received September 3, 1980

The plutonium–oxygen phase diagram has been clarified by XPS and AES results which show that three oxygen-containing plutonium phases, PuO_2 , $\alpha\text{-Pu}_2\text{O}_3$, and PuO_xC_y , are successively formed when oxide-coated plutonium metal is heated in vacuo to 500 °C. Formation of the oxide carbide is evidenced by the fact that a shift in the $\text{Pu}(4f_{7/2})$ binding energy is coincident with changes in the $\text{C}(1s)$ photoelectron and $\text{C}(\text{KLL})$ Auger spectra, showing that unbound carbon is converted to carbide. The reaction conditions duplicate those at which plutonium monoxide reportedly forms and demonstrate that the NaCl-type surface phase previously identified as PuO is actually PuO_xC_y . The oxide carbide has a spectroscopically determined composition of $\text{PuO}_{0.65 \pm 0.15}\text{C}_{0.45 \pm 0.15}$ and reacts with CO , CO_2 , and O_2 at low pressures to form PuO_2 and unbound carbon in a coherent product layer (~ 20 nm thick) which retards further oxidation. Estimated thermodynamic data for PuO_xC_y are consistent with the observed formation and oxidation reactions. The $\text{Pu}(4f_{7/2})$ binding energies for PuO_2 , $\alpha\text{-Pu}_2\text{O}_3$, PuO_xC_y , and Pu are 426.1, 424.4, 423.6, and 422.2 eV, respectively.

Introduction

The phase diagram of the plutonium–oxygen system remains uncertain concerning the existence of condensed plutonium monoxide. Various reports of the NaCl-type ($a_0 = 0.4958 \pm 0.0002$ nm) monoxide are included in early reviews of physicochemical properties of plutonium compounds.^{1,2} The phase diagram recommended by Livey and Feschotte shows that only hexagonal $\beta\text{-PuO}_{1.50}$, cubic $\text{PuO}_{1.515}$, cubic $\text{PuO}_{1.61}$, and cubic $\text{PuO}_{2.00}$ exist at 300 °C.¹ The body-centered-cubic $\text{PuO}_{1.515}$ phase, which is designated as $\alpha\text{-Pu}_2\text{O}_3$, disproportionates into $\beta\text{-PuO}_{1.50}$ and $\text{PuO}_{1.61}$ at approximately 360 °C. The $\text{PuO}_{1.61}$ phase exists only at temperatures above 290 °C and forms a continuous cubic solid solution with $\text{PuO}_{2.00}$ at higher temperatures. However, the high-temperature X-ray diffraction study by Terada et al. shows that three condensed plutonium oxides (PuO_2 , $\alpha\text{-Pu}_2\text{O}_3$ and PuO) are successively formed when the PuO_2 -coated metal is heated to 500 °C in a 10^{-5} Pa vacuum.³

Attempts to prepare bulk quantities of the monoxide by reacting the metal with the higher oxides have failed,^{1,4} and calculations based on estimated thermodynamic data for PuO indicate that these reactions have positive free energy changes.⁵ The monoxide is observed only as a silver layer on the surface of vacuum-heat-treated plutonium and maintains its metallic luster when exposed to air for periods of days or weeks. Some workers have suggested that the phase might be stabilized by impurities such as carbon.^{1,5} Others have maintained that a monoxide layer is stabilized by surface film energies.⁶ Since

such differences of opinion concerning the $\text{Pu} + \text{O}$ system have existed for more than 15 years without resolution, a new approach to the problem is clearly needed.

Results of a recent X-ray photoelectron spectroscopy (XPS) and Auger electron spectroscopy (AES) study of plutonium oxidation at ambient temperature suggest that such surface analysis techniques could be employed to resolve the phase diagram problem.⁷ The present study was initiated to identify the surface phases formed when PuO_2 -coated plutonium is heated in vacuo and to assign their XPS and AES spectra. After data showed that the product formed at the highest temperatures deteriorates when stored in the spectrometer, its interactions with major residual gases (CO and CO_2) in the vacuum system and with O_2 were investigated.

Experimental Section

The spectrometer, specimen, and procedures used in this study are identical with those described in the recent XPS–AES investigation of plutonium oxidation.⁷ XPS and AES spectra were obtained with the use of a double-pass cylindrical mirror analyzer. For the XPS measurements, the 1253.6-eV $\text{Mg K}\alpha$ line was used as the source. Binding energies were calibrated against the $\text{Au}(4f_{7/2})$ peak at 83.8 eV.

The major impurities of the electrorefined plutonium metal sample (in ppm) are as follows: Am, 522; Ga, 107; Fe, 99; Cr, 76; Al, 64; Ta, 60; Ni, 38; Zn, 28; C, 23; Si, 22. The sample surface was cleaned by a combination of Ar^+ bombardment and 500 °C heat treatments. The impurities observed on the surface after cleaning were ca. 10 atom % carbon and 5 atom % oxygen. Tantalum (ca. 8 atom %) was also detected by XPS. Since Ta was not detected by AES and since segregation of Ta to the surface is not to be expected, the XPS spectrum probably originated either from impingement of the incident beam on the Ta sample holder or from excitation of Ta that had been transported from the sample holder to the sample surface during sputtering. The specimen was oxidized at ambient temperature by exposure to 1.8×10^8 L of O_2 . Ellipsometric measurements have shown that a 20-nm thick PuO_2 layer is formed at these conditions.⁸

(1) Livey, D. T.; Feschotte, P. *At. Energy Rev. Spec. Issue* **1966**, *4* (No. 1), 53.

(2) Notwotny, H.; Seifert, K. *At. Energy Rev. Spec. Issue* **1966**, *4* (No. 1), 73.

(3) Terada, K.; Meisel, R. L.; Dringman, M. R. *J. Nucl. Mater.* **1969**, *30*, 340.

(4) Chikalla, T. D.; McNeilly, C. E.; Skavadhl, R. E. Report HW-74802; AEC: Hanford, WA, 1962.

(5) Oetting, F. L. *Chem. Rev.* **1967**, *67*, 261.

(6) Mulford, R. N. R.; Holley, C. E., Jr. Report LA-DC-8266; AEC: Los Alamos, NM, 1966.

(7) Larson, D. T. *J. Vac. Sci.-Technol.* **1980**, *17*, 55.

(8) Larson, D. T.; Cash, D. L. *J. Phys. Chem.* **1969**, *73*, 2814.

Table I. XPS Binding Energies and Fwhm Values Observed during Vacuum Heat Treatment of Oxide-Coated Pu Metal

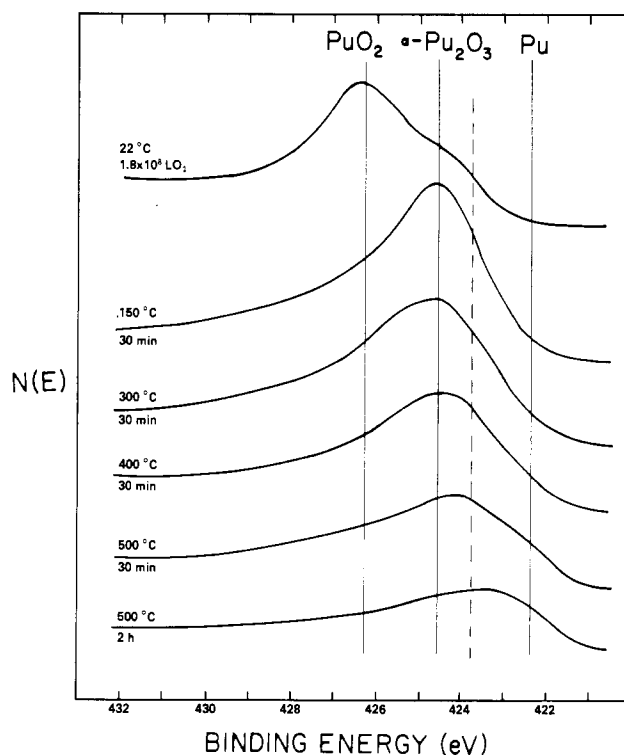
temp, °C	time, min	binding energy, eV			fwhm, eV
		Pu(4f _{7/2})	C(1s)	O(1s)	
22		426.2, 424.3 ^a	284.6	530.1	3.2
150	30	424.4	284.8	530.0	2.8
250	30	424.2	284.2	529.7	3.3
300	30	424.3	284.2	529.9	3.3
400	30	424.3	286.3, 281.1	529.8	3.6
500	30	424.0	280.9	529.7	4.0
500	30	423.7	281.2	530.1	4.1
500	30	424.0	281.2	530.1	4.0
500	120	423.6	281.0	530.1	3.8

^a Shoulder.

High-temperature experiments were performed in situ by electron bombardment heating of the sample mounted between two sheets of 0.25 mm thick tantalum. A 0.20-cm² area of the sample surface was accessible through a hole in the outer sheet. Temperatures up to 500 °C were measured with an uncertainty of ±10% with use of a chromel–alumel thermocouple spot welded to the Ta holder. Spectra were measured after the sample was heat treated at selected temperatures between 22 and 500 °C. During the heating cycles the residual pressure in the vacuum system increased sharply from the ultimate value of 0.1 μPa. At 150 °C the total pressure was 0.7 μPa; the major constituents were 0.3 μPa CO, 0.2 μPa H₂O, and 0.1 μPa CO₂. At 500 °C the partial pressures of CO₂ and CO were 1 and 2 μPa, respectively, and the total residual pressure was 4 μPa.

Several properties of the surface phases formed during heat treatment were measured. Auger energies and XPS binding energies were assigned and determined as described previously.⁷ Complex XPS spectra were resolved into Gaussian peaks by a regression analysis computer program. These procedures provided accurate determinations of the XPS peak areas for specific species. Phase compositions were estimated from the XPS data with use of published atomic sensitivity factors of 0.63 for O(1s), 0.205 for C(1s), and an extrapolated value of 6.4 for Pu(4f_{7/2}).⁹ A 6.4 value was also obtained for Pu from the theoretical values of photoionization cross sections¹⁰ corrected for the dependence of electron mean free path on kinetic energy⁹ and the relationship describing the dependence of the kinetic energy on the detection efficiency of the energy analyzer.¹¹ The phase compositions were determined from the AES data with use of sensitivity factors calculated for O and C (α_O , α_C) relative to Pu. Use of derivative-mode AES data for determining atomic concentrations can lead to errors if the peak shapes change. The 317-eV Pu and 511-eV O peaks were selected because their shapes are the same for all oxygen- and carbon-containing phases. The 272-eV C peak was used for calculating C/Pu ratios only when the oxide carbide phase was present. The average α_O obtained on known oxide phases (α -Pu₂O₃ and PuO₂) using the 511-eV O and 317-eV Pu peaks was 4.6. An average α_C of 4.2 was obtained from the 272-eV C and 317-eV Pu peaks by assuming that the carbide spectrum observed after cleaning the metal and heating at 500 °C corresponds to the metal-rich ($z = 0.33$) boundary of the PuC₁₋₂ phase.^{2,5}

The interactions of the surface phase formed at 500 °C with CO, CO₂, and O₂ were investigated by exposing freshly prepared specimens to the pure gases (>99.99 mol %) at 1.3 Pa pressure for 4 h and remeasuring the spectra. After each gas exposure, the surface was regenerated by heat treatment at 500 °C. Sputter etching with 1 keV of Ar⁺ at 24 μA cm⁻² was utilized to remove adsorbed species and obtain depth profiles. Atomic compositions were calculated with use of the relationship $C_X = (I_X/\alpha_X)/(\sum I_i/\alpha_i)$, where I_X and α_X are the peak intensity and sensitivity factor for atom X, respectively.^{9,12}

**Figure 1.** XPS Pu(4f_{7/2}) spectra from a PuO₂-coated Pu sample after vacuum heat treatment at selected temperatures. (The Pu(4f_{7/2}) binding energies for PuO₂, α -Pu₂O₃, PuO_x, and Pu are 426.1, 424.4, 423.6 and 422.2 eV, respectively.)

Corrections for attenuation of substrate signals by atomic overlayers were made with the exponential relationships described by Chang.¹³

Results

High-Temperature Phases. XPS and AES data show that Pu, O, and C are present and that marked changes in the spectra of these elements are induced by vacuum heat treatment. The behavior of the XPS Pu(4f_{7/2}) peak is shown in Figure 1 and Table I. As shown by the solid line at 426.1 eV in Figure 1, the surface oxide at 22 °C is PuO₂; however, a trace of the unidentified suboxide observed at 424.4 eV in the earlier study is also present.⁷ At 150 °C the surface is completely converted to this suboxide. At 300 °C a low-energy shoulder is evident, and after treatment at 500 °C the Pu(4f_{7/2}) peak is completely shifted to 423.6 eV as indicated by the dashed line in Figure 1. As shown by the results in Table I, the shifts in binding energy are accompanied by changes in the values for the peak width at half-maximum (fwhm).

Assignment of the Pu(4f_{7/2}) spectra of the high-temperature products is facilitated by correlating the results in Figure 1 with the high-temperature X-ray diffraction data reported by Terada et al.³ Since a surface layer of PuO₂ is completely converted to bcc PuO_{1.515} at 150 °C, the suboxide with a 424.4-eV binding energy is α -Pu₂O₃. The previously unobserved 423.6-eV peak is distinctly different from the 422.2-eV binding energy of Pu metal.⁷ However, X-ray data show that α -Pu₂O₃ is allegedly converted to fcc PuO in the 250–500 °C temperature range,³ and the 423.6-eV peak is definitely assignable to that phase.

Insight into the true identity of the high-temperature fcc phase is gained by examining the effects of heat treatment on the XPS and AES spectra of carbon in Figures 2 and 3. Although the broad XPS C(1s) peak observed at 284.6 eV (cf. Figure 2) is coincident with that of hydrocarbons, the peak can also be assigned to the presence of unbound carbon for

(9) Wagner, C. D.; Riggs, W. M.; Davis, L. E.; Moulder, J. F. "Handbook of X-Ray photoelectron Spectroscopy"; Perkin-Elmer Corp.: Eden Prairie, MN, 1979.

(10) Scofield, J. H. *J. Electron Spectrosc. Relat. Phenom.* **1976**, *8*, 129.

(11) Palmberg, P. W. *J. Vac. Sci. Technol.* **1975**, *12*, 379.

(12) Davis, D. E.; MacDonald, N. C.; Palmberg, P. W.; Riach, G. E.; Weber, R. E. "Handbook of Auger Electron Spectroscopy", 2nd ed.; Physical Electronics Industries, Inc.: Eden Prairie, MN, 1976.

(13) Chang, C. C. *Surface Sci.* **1975**, *48*, 9.

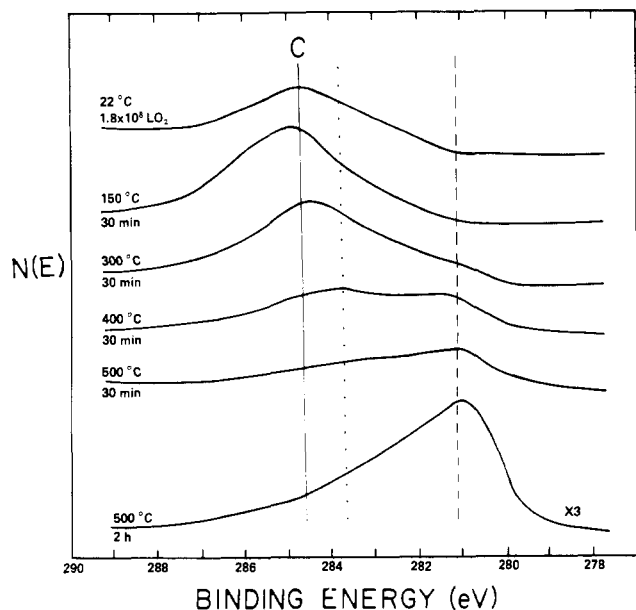


Figure 2. XPS C(1s) spectra from a PuO₂-coated Pu sample after vacuum heat treatment at selected temperatures. (The C(1s) binding energies for unbound C and PuO_xO_y are 284.6 and 281.0 eV, respectively.)

which a binding energy of 284.4 eV is reported.⁹ Careful examination of Figure 2 shows that a second carbon peak at 281.0 eV is evident at 300 °C. Conversion of carbon to the new species at 281.0 eV is essentially complete after 2 h at 500 °C, but the peak asymmetry resulting from a high-energy tail shows that other carbon species are still present. Corresponding data for the C(KLL) peak in Figure 3 also show that substantial changes occur in the AES spectra of carbon as the sample is heated.

The spectroscopic data demonstrate that the high-temperature surface phase which has previously been identified as plutonium monoxide is actually an oxide carbide, PuO_xC_y. The existence of three surface phases during the reaction cycle is entirely consistent with the results of the earlier X-ray diffraction study in which PuO₂, α-Pu₂O₃, and PuO were successively observed. The involvement of carbon in the formation of the last phase is evidenced by the coincident changes in the Pu(4f_{7/2}), C(1s), and C(KLL) spectra over the temperature range at which PuO is reported to form. The 423.6- and 281.0-eV binding energies of Pu and C are assigned to the PuO_xC_y phase. The closeness of the Pu(4f_{7/2}) energies in PuO_xC_y and α-Pu₂O₃ demonstrates that Pu is trivalent in the oxide carbide. The low C(1s) binding energy of the phase suggests the formation of a carbide ion; the measured value is in good agreement with the 280.7-eV energy of HfC.⁹ The AES spectrum for C(KLL) at 500 °C exhibits two lower energy peaks near 255 and 265 eV which are characteristic of metal carbide spectra.¹⁴ The O(1s) binding energy in PuO₂, α-Pu₂O₃, and PuO_xC_y (cf. Table I) is invariant; the (529.9 ± 0.2)-eV value is in good agreement with that reported by Allen and Tucker for UO₂.¹⁵

Brief mention should also be made of evidence for a transient carbide species in the XPS spectrum of carbon at 400 °C (cf. Table I and the dotted line in Figure 2). The 283.6-eV peak which is also evident at 300 °C and after short heating at 500 °C is attributed to the presence of a surface plutonium carbide similar to the uranium phase with a binding energy of 283.9 eV observed by Allen and Tucker.¹⁵ The increase

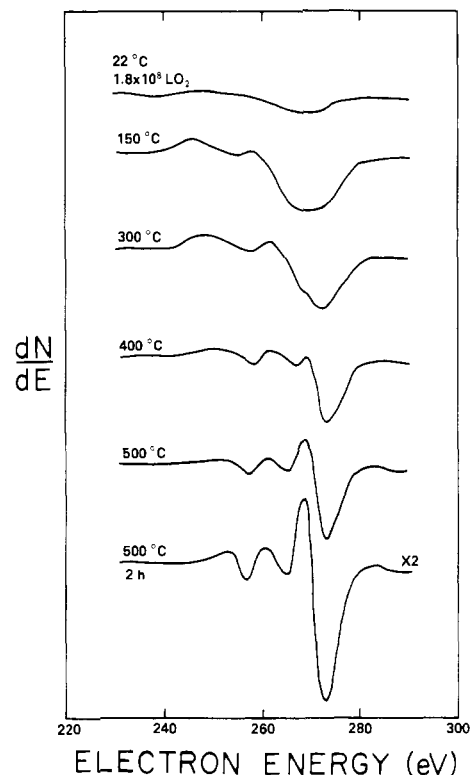


Figure 3. AES C(KLL) spectra from a PuO₂-coated Pu sample after vacuum heat treatment at selected temperatures.

in the fwhm values for Pu(4f_{7/2}) (cf. Table I) in the 300–500 °C range are consistent with the presence of a transient plutonium phase.

Properties of PuO_xC_y. The approximate stoichiometry of the oxide carbide phase has been determined from the observed O/Pu and C/Pu spectral ratios. The observed AES peak-to-peak height ratios and the XPS peak areas are given in Table II. The O/Pu stoichiometries were calculated by a direct procedure and from sensitivity factors. In the direct method, a calibration constant was derived by assuming that the surface stoichiometry at 22 °C was PuO_{2.0}. The resulting value was used to calculate O/Pu ratios for the other conditions. Since use of the published XPS sensitivity factors gave an unreasonably high O/Pu ratio of 3.2 for the dioxide, the data were reevaluated considering the outer surface to be enriched with oxygen. A 0.25 nm thick oxygen layer was assumed to be on the outer surface. The O/Pu and C/Pu ratios obtained before and after this correction are presented in Table II. For PuO_xC_y, the respective average stoichiometries and standard errors derived from the AES and XPS data are PuO_{0.7±0.1}C_{0.4±0.1} and PuO_{0.6±0.1}C_{0.5±0.2}.

Although the characteristic XPS and AES spectra for the oxide carbide are reproducibly obtained by heat treatment of the sample, the product cannot be maintained for extended periods in the spectrometer. In one test PuO_xC_y was prepared, characterized, stored for 22 h in the spectrometer under 0.1 μPa vacuum at room temperature, and then recharacterized. During storage, the XPS Pu(4f_{7/2}) and C(1s) spectra broadened and shifted to higher binding energies, indicating formation of α-Pu₂O₃, some PuO₂, and the transient carbide species with C(1s) at 283.6 eV; however, the spectra showed that PuO_xC_y was still prevalent. Since CO, CO₂, and H₂O are the major residual gases in the system, it is reasonable to assume that degradation of the product is promoted by interaction with these gases.

Results of separate tests in which PuO_xC_y samples were exposed to CO, CO₂, and O₂ at 1.3 Pa for 4 h confirm that they oxidize the oxide carbide. In Figure 4, the C(1s) spectrum

(14) Chang, C. C. "Characterization of Solid Surfaces"; Plenum Press: New York, 1974; Chapter 20, p 509.
 (15) Allen, G. C.; Tucker, P. M. *J. Chem. Soc., Dalton Trans.* 1973, 5, 470.

Table II. Spectral and Calculated Stoichiometric Ratios from AES and XPS Data during Heat Treatment of PuO₂-Coated Pu

temp, °C	Auger electron spectroscopy						X-ray photoelectron spectroscopy						
	calcd stoichiometric ratios						calcd stoichiometric ratios						
	exptl spectral ratios ^a		calibration constant (22 °C PuO _{2.0}) ^b	sensitivity factors		exptl spectral ratios	calibration constant (22 °C PuO _{2.0}) ^b	atomic sensitivity factors					
	O/Pu	C/Pu		O/Pu	C/Pu			O/Pu	C/Pu	O/Pu ^c	C/Pu ^c		
22	9.8	<i>d</i>	2.0	2.1	0.318	<i>d</i>	2.0	3.2	2.3				
150	6.7	<i>d</i>	1.4	1.5	0.176	<i>d</i>	1.1	1.8	1.2				
250	5.8	<i>d</i>	1.2	1.3	0.132	<i>d</i>	0.8	1.3	0.9				
300	5.5	<i>d</i>	1.1	1.2	0.154	<i>d</i>	1.0	1.6	1.1				
400	4.9	1.4	1.0	1.1	0.143	0.012	0.9	1.5	0.8	0.4	0.3		
500	3.7	1.6	0.8	0.8	0.129	0.010	0.8	1.3	0.7	0.3	0.3		
500	2.6	1.4	0.5	0.6	0.081	0.027	0.5	0.8	0.5	0.8	0.7		
500	3.8	1.5	0.8	0.8	0.138	0.023	0.9	1.4	0.8	0.7	0.6		
500	3.4	1.9	0.7	0.7	0.093	0.018	0.6	0.9	0.5	0.6	0.5		

^a For AES the ratios are O(511eV)/Pu(317eV) and C(272eV)/Pu(317eV); for XPS the ratios are O(1s)/Pu(4f_{7/2}) and C(1s)/Pu(4f_{7/2}). ^b The O/Pu ratios are based on the assumption that the spectral ratio at 22 °C corresponds to an O/Pu ratio of 2.0, i.e., that the surface phase is pure PuO₂. ^c Values are corrected assuming outer oxygen atomic layer with thickness of 0.25 nm. ^d Free carbon or intermediate carbide is present.

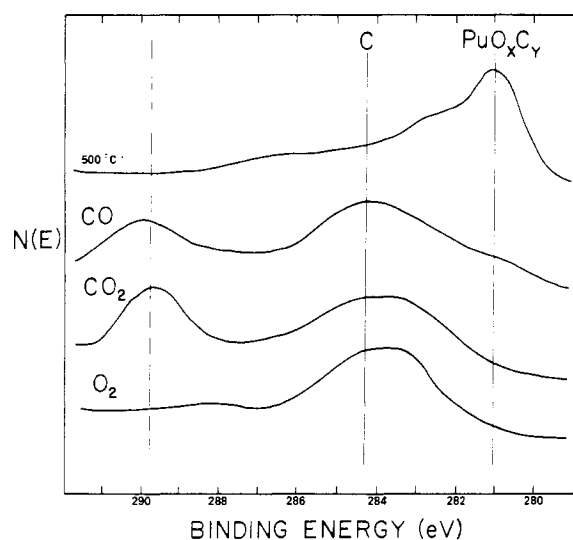


Figure 4. Comparison of the XPS C(1s) spectrum of a freshly prepared PuO_xC_y sample with those obtained after exposure of the oxide carbide to CO, CO₂, and O₂ at 1.3 Pa pressure for 4 h at room temperature.

of freshly prepared PuO_xC_y is compared with those obtained after exposure. In all cases the oxide carbide spectrum disappears and carbon is converted to unbound carbon (284.4 eV) or to a mixture of unbound carbon and the surface carbide (283.6 eV). A particularly interesting feature of the spectra for CO and CO₂ is the presence of a new higher energy carbon peak at 289.7 ± 0.2 eV. Parallel XPS data for Pu(4f_{7/2}) in Figure 5 show that the production of free carbon is accompanied by formation of plutonium oxides. A mixture of α-Pu₂O₃ and PuO₂ is apparently formed by CO and CO₂; however, only PuO₂ is detectable after O₂ exposure.

Although the invariant 530-eV peak of the plutonium oxide phases is present in the O(1s) spectra (cf. Figure 5), the data for CO and CO₂ show a new oxygen peak at 532.0 ± 0.2 eV. The new carbon and oxygen peaks accompanying CO and CO₂ treatment are attributed to adsorbed carbon-oxygen species on the PuO₂ surface. These species are removed from the surface by either sputter etching to 5-nm depth or heating to 500 °C. The binding energies of the species are similar for both gases, but the O/C ratios (2.3 for CO and 5.3 for CO₂) obtained directly from peak areas and sensitivity factors suggest that the species are different. Since the 289.7-eV C(1s) binding energy is lower than the 291.8- and 290.2-eV values for CO₂ and CO,⁹ respectively, the electron density on the

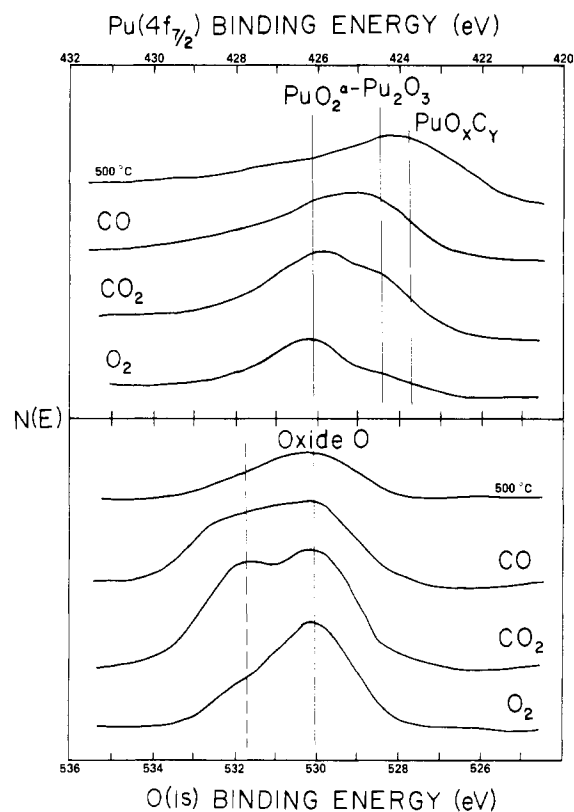


Figure 5. Comparison of the XPS Pu(4f_{7/2}) (upper set) and O(1s) (lower set) spectra of freshly prepared PuO_xC_y with those obtained after exposure of the oxide carbide to CO, CO₂, and O₂ at 1.3 Pa pressure for 4 h at room temperature.

carbon atom of the species is apparently increased by the adsorption process. This observation is consistent with formation of a negatively charged carbon oxide such as carboxylate, CO₂⁻, observed by Colmenares on p-type UO_{2+x}¹⁶ and assumed to be present on p-type PuO₂.¹⁷ If carboxylate is present and oriented as proposed by Colmenares,¹⁶ the outer atomic layer is entirely oxygen and the second layer is carbon. Correction of the XPS data for the presence of a 0.25 nm thick oxygen layer gives O/C ratios of 1.6 and 3.7 for the adsorbed species on CO- and CO₂-treated samples, respectively.

(16) Colmenares, C. A. *J. Phys. Chem.* **1974**, *78*, 2117.

(17) Colmenares, C. A.; Terada, K. *J. Nucl. Mater.* **1975**, *58*, 336.

Table III. Depth Profile Data for PuO_xC_y Sample after O₂ Exposure

depth ^a nm	AES stoichiometry		XPS binding energy, eV			fwhm, eV Pu(4f _{7/2})
	O/Pu	C/Pu ^b	Pu(4f _{7/2})	C(1s)	O(1s)	
0	2.1	0.08	426.0	283.6, 284.6	530.1	2.6
10	0.9	0.3	424.6	282.4, 284.7	530.1, 531.6	3.2
20	0.7	0.3	424.3	282.3	530.0, 531.8	4.3
40	0.6	0.4	c	c	c	c
60	0.6	0.3	c	c	c	c
100	0.5	0.4	423.7	282.1	530.2	4.8
150	0.5	0.3	c	c	c	c
200	0.4	0.3	423.2	281.9	530.3	4.6
300	0.4	0.3	c	c	c	c
500	0.3	0.2	422.4	281.6	530.5	4.4

^a A sputter etch rate of 1.6 nm/min for the plutonium oxide was calibrated with use of ellipsometric thickness data and identical sputter parameters for a UO₂ layer on U. ^b AES carbon peak a mixture of free carbon and carbide. ^c XPS spectra not measured.

The nature of the products formed by treatment of PuO_xC_y with CO, CO₂, and O₂ has been further characterized by sputter etching. As an example, the depth profile results for an O₂-treated sample are presented in Table III. Both the XPS and AES data show that the outer layer is PuO₂. The Pu(4f_{7/2}) energies show that α-Pu₂O₃, PuO_xC_y, and Pu appear in succession during etching. The stoichiometry and binding energies for depths of 20–100 nm are consistent with the presence of unreacted PuO_xC_y; the thickness of this layer is in good agreement with the 80-nm depth expected to result from reaction of a 20-nm thick PuO₂ layer. The C(1s) binding energy of 282 eV suggests a mixture of oxide carbide (281.0 eV) and transient carbide (283.6 eV), but the effects of sputtering on the surface properties and spectra are difficult to assess. Sputtering is known to form carbides from carbon contaminants, reduce oxide phases, cause the surface composition to change because of different sputtering rates of the elements, and drive atoms deeper into the surface.^{18,19}

Discussion

XPS and AES data for samples prepared under conditions known to produce PuO show that the so-called monoxide is actually an oxide carbide, PuO_xC_y. The experimental evidence from the present study and from earlier work is overwhelming. The investigation of the Pu–O–C system by Mulford et al. shows that an anion-deficient NaCl-type oxide carbide of variable composition exists between PuC_{0.86±0.04} and PuO_{0.54}C_{0.38} and that the most oxygen-rich composition has a lattice parameter in the range 0.4958 ± 0.0002 nm.²⁰ The oxide carbide parameter agrees exactly with that reported for PuO;² the PuO_xC_y composition determined from AES and XPS data (PuO_{0.65±0.15}C_{0.45±0.15}) is in surprisingly good agreement with that of the oxygen-rich oxide carbide. These observations, the spectroscopic evidence for the simultaneous conversion of unbound carbon to carbide during vacuum heat treatment, and the fact that the characteristic electron spectra of the product do not appear when clean metal is slowly oxidized⁷ all indicate that the surface phase is the oxide carbide and not the monoxide.

Several potential sources of the carbon required for formation of PuO_xC_y have been identified. Results of the previous

study with plutonium showed an inherent carbon contamination that could not be removed by sputter etching and heat treatment.⁷ The present study indicates that both unbound carbon and plutonium carbide react with Pu₂O₃ and Pu to form oxide carbide. Unbound carbon may result from pyrolysis of hydrocarbons on the surface, but the most likely mechanism for introducing additional carbon into a plutonium sample is the interaction of reduced surface phases with CO and CO₂. We have demonstrated that these gases oxidize PuO_xC_y and Pu₂O₃ to form PuO₂ and C. Similar reactions are expected to occur with plutonium metal.

Recognition of the potential carbon sources facilitates understanding of the fact that only thin (<1 μm) layers of the product are formed by heat treatment. This behavior is attributed to the limited availability of carbon at the oxide-coated surface. The formation of oxide carbide proceeds at a rapid rate until all the carbon or carbide at the surface is consumed. If the reaction is reagent limited by the availability of carbon, formation of the most oxygen-rich PuO_xC_y phase is expected. The close agreement between the composition and lattice parameter of the surface product and those of the oxygen-rich oxide carbide observed by Mulford et al.²⁰ is readily understood.

The primary conclusion of the present study is consistent with that of an early XPS investigation of surface oxidation of uranium.¹⁵ The behavior of U(4f_{7/2}), O(1s), and C(1s) energies during heat treatment closely parallel our results for plutonium; however, the authors conclude the "UO is stabilized by the presence of uranium carbide", not that UO_xC_y is formed. Their results are in marked contrast to those of Ellis, who used "very clean" surfaces with no detectable impurities and concluded that UO is a stable surface species at elevated temperatures.²¹ When the sample was heated to 700 °C, the AES signal of oxygen was found to be half that observed for UO₂. That spectrum was preserved on cooling the sample to room temperature but was irreversibly destroyed by heating to 800 °C. Since CO was also the major residual gas during the tests, introduction of carbon contamination from that source cannot be excluded. Additional work is needed to resolve the uranium monoxide question.

The properties of the PuO_xC_y phase closely parallel those of the NaCl-type rare-earth oxide carbides.^{22–24} In fact the phase that was originally identified as YbO is actually YbO_{0.50}C_{0.47},²³ and recent results suggest that SmC_{0.33} is SmO_{0.51}C_{0.38}.²⁴ Samarium is frequently employed as a model for plutonium, and a very close correspondence is found in the present case. The composition of the samarium oxide carbide is in excellent agreement with that of the oxygen-rich plutonium phase (PuO_{0.54}C_{0.38}).²⁰ Both Sm and Pu are trivalent in their oxide carbides, and both have a silver luster and metallic appearance. By analogy to the rare-earth phases,^{22–24} the carbon species is probably methanide; i.e., hydrolysis of PuO_xC_y generates methane. The metallic properties of PuO_xC_y are attributed to a conduction-band electron population induced by anion deficiency.²⁴

Two important differences between the samarium and plutonium oxide carbides are observed. PuO_xC_y forms an extended solid solution,²⁰ but the samarium phase is stoichiometric with a composition near that of the most oxygen-rich plutonium phase. The absence of a samarium monocarbide phase precludes the existence of a solid solution like that of PuO_xC_y. Although samarium oxide carbide is extremely reactive with air, PuO_xC_y retains its metallic luster and integrity after extended air exposure. The thin (~20 nm)

(18) Holm, R.; Storp, S. *Appl. Phys.* **1977**, *12*, 101.

(19) Wehner, G. K. "Methods of Surface Analysis"; Elsevier: New York, 1975; Vol. 1, Chapter 1, p 5.

(20) Mulford, R. N. R.; Ellinger, F. H.; Johnson, K. A. *J. Nucl. Mater.* **1965**, *17*, 324.

(21) Ellis, W. P. *Surface Sci.* **1976**, *61*, 37.

(22) Butherus, A. D.; Eick, H. A. *J. Am. Chem. Soc.* **1968**, *90*, 1715.

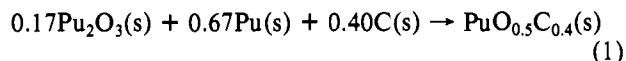
(23) Haschke, J. M.; Eick, H. A. *Inorg. Chem.* **1970**, *9*, 851.

(24) Haschke, J. J.; Deline, T. A. *Inorg. Chem.* **1980**, *19*, 527.

surface layer of oxide formed on PuO_xC_y by oxidizing gases is apparently very coherent and functions as an effective diffusion barrier against extensive reaction.

A dearth of thermochemical data has long hindered resolution of questions about the existence of condensed PuO. Although that situation is not directly improved by the results of this study, the thermodynamic values estimated for PuO^5 definitely cannot be applied to PuO_xC_y . Only the C_p values and the enthalpy increments estimated for the monoxide are valid. Since data are insufficient for a Born-Haber calculation, enthalpy of formation estimates have been used on the analogy of PuO_xC_y to $\text{SmO}_{0.51}\text{C}_{0.38}$ and to PuN . Since the compositions of the Sm and Pu phases are virtually identical, $\Delta H_f^\circ_{298}[\text{PuO}_x\text{C}_y(\text{s})]$ should be similar to the -370 kJ mol^{-1} value of samarium oxide carbide.²⁵ Plutonium nitride is isostructural and isoelectronic with the oxide carbide, and $\Delta H_f^\circ_{298}[\text{PuN}(\text{s})] = -317 \text{ kJ mol}^{-1}$.⁵ The average estimated $\Delta H_f^\circ_{298}[\text{PuO}_x\text{C}_y(\text{s})]$ obtained from the values for these model phases is $-344 \pm 35 \text{ kJ mol}^{-1}$. $S^\circ_{298}[\text{PuO}_x\text{C}_y(\text{s})]$ has been obtained with use of Latimer's method with lattice contributions of 67, 0, and $-16 \text{ J K}^{-1} \text{ mol}^{-1}$ for Pu, O, and C.²⁵⁻²⁷ Inclusion of a magnetic contribution similar to that of trivalent samarium ($14.6 \text{ J K}^{-1} \text{ mol}^{-1}$)²⁷ gives an estimated $S^\circ_{298}[\text{PuO}_x\text{C}_y(\text{s})]$ of $75 \text{ J K}^{-1} \text{ mol}^{-1}$ and in conjunction with S°_{298} data for the elements^{5,28} leads to values of $\Delta S_f^\circ_{298}[\text{PuO}_x\text{C}_y(\text{s})] = -33 \pm 5 \text{ J K}^{-1} \text{ mol}^{-1}$ and $\Delta G_f^\circ_{298}[\text{PuO}_x\text{C}_y(\text{s})] = -334 \pm 38 \text{ kJ mol}^{-1}$.

The thermodynamic estimates are consistent with the reactions observed in this study. As previous investigators have noted, PuO should be thermodynamically unstable relative to Pu_2O_3 and Pu.³ However, ΔG°_{298} for the formation of PuO_xC_y according to eq 1 is -63 kJ mol^{-1} . This result, which is derived



from the estimated $\Delta G_f^\circ_{298}$ of $\text{PuO}_x\text{C}_y(\text{s})$ and from that of Pu_2O_3 ,⁵ supports our conclusions that the NaCl-type surface

phase is the stable oxide carbide and that its thickness is determined by the availability of carbon. The data are also consistent with the proposed formation of a transient plutonium carbide phase that ultimately reacts to form PuO_xC_y . Free energy calculations for the reaction of known carbides with the oxide and metal show that all possible processes are spontaneous.

The reactions of PuO_xC_y with CO , CO_2 , and O_2 to form $\text{PuO}_2(\text{s})$ plus $\text{C}(\text{s})$ are also spontaneous. The least favorable of these processes is given by eq 2 and has $\Delta G^\circ_{298} = -373 \text{ kJ}$

$$\text{PuO}_{0.5}\text{C}_{0.4}(\text{s}) + 0.75\text{CO}_2(\text{g}) \rightarrow \text{PuO}_2(\text{s}) + 1.15\text{C}(\text{s}) \quad (2)$$

mol^{-1} .^{5,28} The ΔG_{298} values for eq 2 with the partial pressures that were present during CO_2 treatment (1.3 Pa) and during exposure to residual CO_2 (10 nPa) are -360 and -297 kJ mol^{-1} , respectively. Equation 2 and the parallel reaction for CO are particularly important because they provide a mechanism for increasing the surface concentration of carbon on plutonium.

The present study supports a Pu-O phase diagram in which the condensed monoxide does not exist at standard conditions. However, recent studies with the rare earths at high pressures (40-80 GPa) and high temperatures (600-1200 °C) show that several elements (La-Nd, Sm) react with their higher oxides to form metallic NaCl-type monoxides and that Yb forms a nonmetallic monoxide.²⁹ These rare earths are similar to Pu in that their condensed monoxides are unstable at standard conditions. Although the known high-temperature surface phase is definitely PuO_xC_y , it is reasonable to assume that the synthesis of PuO can be achieved by similar high-pressure techniques.

Acknowledgment. This work was performed under DOE Contract DE-AC04-76DP03533. We wish to thank G. E. Bixby for preparing the Gaussian regression analysis computer program used in data analysis.

Registry No. Pu, 7440-07-5; O_2 , 7782-44-7; PuO_2 , 12059-95-9; $\alpha\text{-Pu}_2\text{O}_3$, 12036-34-9; PuO, 12035-83-5; PuC, 12070-03-0; CO, 630-08-0; CO_2 , 124-38-9.

(25) Haschke, J. M., to be submitted for publication.

(26) Latimer, W. M. *J. Am. Chem. Soc.* **1951**, *73*, 1480.

(27) Westrum, E. F., Jr. *Adv. Chem. Ser.* **1967**, *No. 71*, p 25.

(28) "JANF Thermochemical Tables", *Natl. Stand. Ref. Data Ser. (U.S. Natl. Bur. Stand.)* **1971**, *NSRDS-NBS 37*.

(29) Leger, J. M.; Yacoubic, N.; Loriers, J. "The Rare Earths in Modern Science and Technology"; Plenum Press: New York, 1980; Vol. 2, p 203.

Contribution from the Department of Physical Chemistry, Åbo Akademi, SF-20500 Åbo (Turku), Finland, and the Department of Chemistry, University of Michigan, Ann Arbor, Michigan 48109

Relativistically Parameterized Extended Hückel Calculations. 3. Structure and Bonding for Some Compounds of Uranium and Other Heavy Elements

P. PYYKKÖ and L. L. LOHR, JR.*

Received September 16, 1980

The relativistically parameterized extended Hückel molecular orbital method REX is used to explore the effects of relativity upon molecular orbital energies and compositions. The uranium compounds studied are UO_2^{2+} , $\text{UO}_2\text{Cl}_4^{2-}$, UF_6 , UCl_6 , UCl_4 , $\text{U}(\text{BH}_4)_4$, and $\text{U}(\text{C}_6\text{H}_8)_2$. Other heavy element compounds studied are MI_3 ($\text{M} = \text{La, Gd, Lu}$), PoH_2 , $(\text{eka})\text{PoH}_2$, I_3^- , AtI_2^- , and RnF_2 . Relativistic orbital energy parameters and atomic orbital exponents are presented as supplementary material for all elements with $Z = 1-120$ together with corresponding nonrelativistic values for all elements with $Z = 1-100$. It is concluded that the REX method provides semiquantitative estimates of spin-orbit splittings and relativistic bonding effects for compounds of heavy elements.

Introduction

In a recent publication,¹ referred to hereafter as part 1, we outlined a relativistically parameterized version of extended Hückel theory (EHT) called REX. This method incorporates

relativistic effects by its use of atomic orbital basis sets with an $|lsjm\rangle$ quantization and by its systematic parameterizations based on Desclaux' atomic relativistic Dirac-Fock (DF) and nonrelativistic Hartree-Fock (HF) calculations.² No spin-orbit Hamiltonian need be specified, as the diagonal Hamil-

* To whom correspondence should be addressed at the University of Michigan.

(1) L. L. Lohr, Jr., and P. Pyykkö, *Chem. Phys. Lett.*, **62**, 333 (1979).
(2) J. P. Desclaux, *At. Data Nucl. Data Tables*, **12**, 311 (1973).